telecom

MDPI

Article

Anti-Skid Aircraft Braking Mechanism Using Consensus Control over Wireless Avionic Intra-Communication

Zohaib Ijaz [1,2,*], Fadhil Firyaguna [3] and Dirk Pesch [2]

[1] Regulated Software Research Centre (RSRC), Department of Computer Science and Mathematics, Dundalk Institute of Technology, A91 K584 Dundalk, Ireland
[2] School of Computer Science & IT, University College Cork, T12 K8AF Cork, Ireland; dirk.pesch@ucc.ie
[3] Collins Aerospace, Applied Research & Technology, T23 XN53 Cork, Ireland; fadhil.firyaguna@collins.com
* Correspondence: zohaib.ijaz@dkit.ie

Abstract

This article discusses the anti-skid braking control mechanism of aircrafts. Aircrafts use a sliding-mode controller (SMC) to generate the desired braking torque on its wheels to stop while landing. Potential runway variations and load differences on the wheels are considered, affecting the friction force on each wheel. Variations in the friction force generate drag torque, causing aircrafts to drift away from the runway. In order to counteract the drift, we propose a supervisory consensus controller, which adjusts the braking torque of each wheel to achieve equal force on each wheel. We consider a wireless communication channel between the supervisory controller and each wheel's brake controller in an attempt to reduce cabling. As wireless communication needs to deal with potential communication losses that affect the overall control performance, a new control model that can accommodate communication losses has been devised. The proposed model is evaluated, and we demonstrate how well the consensus controller works over a noisy channel. Simulation results demonstrate that the proposed consensus-based control significantly improves braking performance, reducing drag torque and achieving up to 15–20% reduction in landing distance under 25% packet loss compared to baseline approaches.

Keywords: anti-skid; consensus control; runway variations; drag torque on aircraft; sliding-mode control; packet loss; noisy channel

1. Introduction

The next generation of commercial aircraft is being developed to provide more reliable, cost-efficient, and safer flights. Part of this effort is introducing the wireless avionics intra-communications (WAIC) system [1]. This system aims to reduce aircraft weight by replacing wired with wireless systems, as cabling and wiring present a significant cost associated with an aircraft's fabrication, maintenance, and weight. A particular advantage of a wireless system is the operational enhancement of landing gear sensors (wheel speed for anti-skid control and position feedback for steering), as it provides increased flexibility for monitoring moving and rotating parts. These landing gear functions send important status information in real-time to keep the flight's high levels of reliability and safety.

In this context, a landing gear control system operating over a wireless sensor network must be at least as reliable as one operating over a traditional wired network. However, the wireless environment poses a different challenge for connection reliability where communication is performed in a shared medium (over the air), causing radio interference

Check for updates

Academic Editor: Barbara M. Masini

Received: 1 April 2026
Revised: 6 May 2026
Accepted: 8 May 2026
Published: 13 May 2026

Copyright: © 2026 by the authors. Licensee MDPI, Basel, Switzerland. This article is an open access article distributed under the terms and conditions of the Creative Commons Attribution (CC BY) license.

from other systems (e.g., radio-altimeters, other WAIC devices or networks), which can cause packet losses and transmission delays. Therefore, wireless communication protocols need to be considered to mitigate those effects; at the same time, the design of the landing gear control systems needs to consider the limitations of such communication protocols.

Another critical factor for enhancing a flight's cost-efficiency is ensuring the shortest possible landing distance. The challenge here is the deceleration, where various forces (e.g., air resistance, reverse thrust) are used to stop the aircraft, including the landing wheel braking force, which, if applied too hard, may cause the aircraft to skid and cause an accident [2]. This braking force is heavily dependent on runway friction, which changes dramatically with even minor changes in the weather, such as a few drops of rain or snow [3]. As a result, an anti-skid brake control mechanism is used to maximize the available braking resources. The maximum force that can be applied to the wheel without skidding is determined in the anti-skid brake control model by using the friction of the runway surface [4].

The slip ratio can be used to regulate the friction coefficient. A local sliding-mode controller (SMC) is used to control/regulate the slip ratio of each wheel to the desired value [5]. SMC is an inexpensive control strategy, simple in design, easy to implement, rejects disturbances, and avoids the wheels getting locked in extreme conditions [6]. The friction force available to the wheels changes due to changes in runway conditions, and the braking force applied to the main landing gear may differ for different wheels. This requires the SMC at each wheel to be tuned to achieve equal braking force at each wheel, as uneven forces applied to each wheel cause a drag on the aircraft while landing [7].

To achieve equal braking force, we use a consensus control mechanism similar to consensus of multi-agent systems, in which only the connected neighbors (wheels) can communicate with each other to reach consensus on their braking force exerted on the wheels. A consensus control mechanism (flexible in operation, fault-tolerant, and simple to design) in which the friction coefficient available to each wheel in the main landing gear must be equal. In this consensus control mechanism, all the wheels will communicate with their connected neighbors to exchange information about the friction exerted on each wheel and adjust their desired slip ratio so that all the wheels have the same force on each wheel to keep the aircraft following the path of the runway in the presence of uncertain changes in runway conditions.

To develop a consensus, all neighboring wheels exchange their state information with each other, which eventually reaches the consensus controller. The consensus controller then estimates the friction force based on the received information and communicates it back to the wheels, while most of the existing literature on consensus control assumes perfect communication, in more recent developments using wireless systems, communication noise and uncertainties can degrade the performance of the consensus controller.

Existing anti-skid braking systems models mostly rely on centralized control architectures and assume reliable wired communication. However, emerging wireless avionics intra-communication (WAIC) systems introduce non-negligible communication uncertainties, including delays, interference, and packet loss, while consensus control has been widely studied in multi-agent systems, its application to safety-critical aircraft braking under wireless constraints remains largely unexplored. Particularly, the prior works either neglect communication impairments or assume ideal links. This motivates the need for a control–communication co-design framework that ensures coordinated braking performance under realistic wireless conditions.

In this paper, we analyze the effect of the wireless system and propose a simple communication protocol that helps mitigate the interference and noise uncertainty and coordinates sensor data transmissions between the different wheels. We also propose an

estimation tool to minimize the effects of losing information due to packet loss. Following this, we investigate the impact of communication disruptions over the wireless channel on the overall supervisory control performance. The following are the main contributions of this paper:

- A supervisory consensus control algorithm to regulate the desired slip ratio of each wheel such that the longitudinal force available to each wheel will become equal. The estimated desired slip ratio is fed forward to the SMC at each wheel to generate an equal braking torque that will be exerted on the wheel.
- A wireless communication protocol for consensus control, using a carrier-sensing mechanism to avoid interference, time-slot scheduling to coordinate the transmissions, and the estimation of missing information.
- Investigate the impact of communication uncertainties on the performance of consensus control over the system.

The remainder of this paper is organized as follows: We list and discuss related work in Section 2. The anti-skid brake control model is discussed in Section 3. In Section 4, the supervisory consensus control model is presented. Our wireless communication channel model is developed in Section 5. We present and discuss simulation results in Section 6 and conclude with Section 7.

2. Related Work

The operation of aircraft landing gear is reviewed in [8,9], where the articles survey and highlight the different problems of vibration and oscillations in aircraft due to braking. The anti-skid control landing gear of an aircraft is discussed in [4], where the authors have validated the anti-skid model with some experimental results. A mixed slip and sliding-mode control-based anti-skid model is discussed in [10], in which the authors use sliding-mode observer-based control to estimate the aircraft's speed. The relation between anti-skid controller parameters and braking actuators is discussed in [11], in which the controller set-point is analyzed concerning the total lifespan of wear dynamics. A fuzzy-logic-based anti-skid model is designed to suppress the effect of faults and disturbances in the controller while braking in [12]. An extended stiffness-based runway maximum friction method is proposed in [13] to determine the maximum friction available. The aircraft will operate at the maximum available friction on the wheel.

The current literature has discussed the anti-skid model of the aircraft, but the work needs to consider the sudden change in runway conditions. In reality, the friction force changes with runway conditions. Therefore, there is a need for a certain level of consensus among the wheels of the main landing gear so that, if the surface conditions change, the consensus controller will automatically adjust the slip ratio for each wheel so that all wheels have the same forces acting on them. Consensus control of multi-agent systems has been introduced in [14], where different consensus constraints and typologies of multi-agent systems are discussed. Average consensus algorithms are discussed in [15–18], where all agents connected to a system will reach a common value, which is the average of their initial state values. On the other hand, a leader–follower-based consensus control mechanism is discussed in [19–22], where one of the agents acts as a leader, which will dictate the value that all the followers have to reach.

However, the preceding literature on consensus control has yet to account for communication uncertainties. Perfect communication has been assumed between the agents with no communication delays or uncertainties [14–22]. Recently, some works considered wireless channel communication uncertainties. In [23], the authors discuss consensus control with random packet loss and delays and calculate the upper bound on the delays. Simple non-identical packet loss is mentioned in [24], whereas random packet loss for an

event-based consensus controller was introduced in [22]. In [25], recent advancements on fault-tolerant aircraft brake control systems are discussed. It also highlights the importance of safety-critical systems. Whereas [26] discussed the emerging trends in AI-enabled aviation systems. In [27], the authors discussed communication delays for a consensus controller as a denial of service attack, where the attack can be seen as a communication loss. A time-varying delay-based consensus control scheme is discussed in [28]. In prior literature, authors have studied the impact of random losses and delays on the system. However, they have not discussed the effect of wireless communication protocol design and radio interference intensity in a wireless avionics environment. Actual packet losses in wireless avionics environments differ from those modelled or predicted by consensus control in the current literature. Previous works do not deal with packet loss, and as the proposed system is time-critical, retransmission is not a viable option in this particular case. Therefore, we offer an estimation-based solution to packet losses in this work.

To understand the difference between existing work and our work, the following comparison is presented in Table 1.

Table 1. Comparison of this work with the existing literature.

Work	Anti-Skid Control	Consensus	Wireless	Packet Loss Handling	Application
[4,10]	✓	×	×	×	Aircraft braking
[14–22]	×	✓	×	Limited	Multi-agent systems
[23,24,27,28]	×	✓	Partial	✓	Networked systems
This work	✓	✓	✓ (WAIC)	✓ (estimation)	Aircraft braking

3. Mathematical Model for Anti-Skid Brake Control

3.1. Aircraft Dynamics

When the aircraft touches the ground, the plane experiences a drag torque during landing due to different forces acting on the main landing gear. The torque will impact the momentum over the plane and is defined as

$$J_a \dot{\omega}_a = T_a \tag{1}$$

where J_a is the moment of inertia of the plane and $\dot{\omega}_a$ is the angular acceleration of the plane. T_a is the torque acting on the plane while landing and is defined as

$$T_a = F_l l_l - F_r l_r \tag{2}$$

where F_l, F_r are the forces acting on the left and right landing gears, respectively, and l_l, l_r are the distances of the landing gears from the central axis of the plane as shown in Figure 1. Ideally, to keep the aircraft in a straight direction and follow the central axis of the plane, T_a needs to be zero, which is only possible if $F_l = F_r$, since l_l generally is equal to l_r.

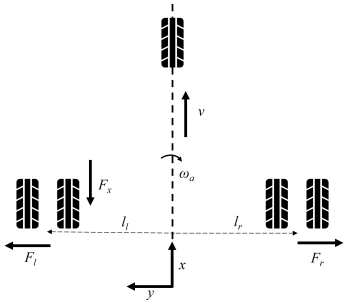


Figure 1. Top view of an airplane.

3.2. Wheel Dynamics

The wheel dynamics need to be studied to obtain F_l, F_r since these forces depend on the friction exerted on aircraft wheels touching the ground. Therefore, in this section, the wheel dynamics of the aircraft are defined with the help of Newton's laws of mechanics [29]. The Newtonian law of conservation of the linear momentum of constant-mass motion (along the x-axis) states that the sum of all the forces acting on the aircraft equals the acceleration times the plane's mass as shown in Equation (3). The wheel dynamics and the forces acting on the wheel are shown in Figure 2.

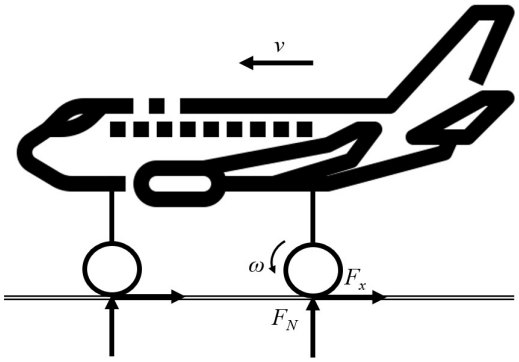


Figure 2. Wheel dynamic model while braking.

$$aM_a = \sum_i F_i \tag{3}$$

where M_a is the mass of the aircraft and a is the acceleration (rate of change of velocity, $\frac{dv}{dt} = a$). Multiple forces act on the aircraft, like drag, rolling, etc., but they are minimal compared to the longitudinal force F_x perpendicular to the normalized force acting on the wheel. Therefore, Equation (3), will become

$$M_a \frac{dv}{dt} = -F_x \tag{4}$$

where F_x is the longitudinal force exerted on the wheel, which is the product of friction available at the wheel and the normalized force action on the wheel (see Figure 3), and represented as

$$F_x = \mu(a, b, \lambda) F_N \tag{5}$$

where μ is the friction coefficient (discussed in the next section), which is a function of the slip ratio λ, the tyre sideslip angle a (the angle between the tyre longitudinal axis and the speed vector of the contact point), and the camber angle b (the tyre inclination for the vertical direction). In this work, both the sideslip angle a and camber angle b are assumed to be zero, which is a common assumption in longitudinal anti-skid braking analysis under nominal landing conditions. During landing rollout, lateral dynamics are typically stabilized by separate control systems (e.g., rudder and nose wheel steering). Therefore, the dominant factor affecting braking performance is the longitudinal slip ratio. This simplification allows us to focus on the interaction between braking coordination and communication constraints. $F_N = M_a g/n$ is the normalized force acting on the wheel of the aircraft. M_a is the loaded weight of the aircraft, and each wheel experiences a different M_a due to the difference in load on each wheel while landing; g is the gravitational constant, and n is the number of wheels (nose and main landing gear) on an aircraft. The longitudinal force F_x in Equation (5), is also known as the *magic formula*, with parameters shown in Figure 3.

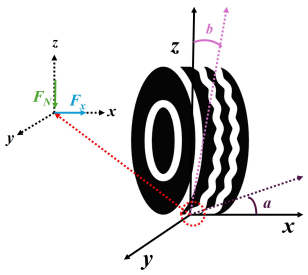


Figure 3. Wheel–runway contact forces.

The law of conservation of angular momentum around the wheel yields

$$J_w \frac{d\omega}{dt} = rF_x - T_b \tag{6}$$

where J_w is the moment of inertia of the wheel, r is the radius of the wheel, and T_b is the braking torque applied to the wheel. We will design in the next subsection the controller to control the slip ratio λ such that the required braking torque T_b is generated, and for the sake of controller design, the sideslip and camber angle are assumed to be small in this work, i.e., $a \approx 0$ and $b \approx 0$. Therefore, $\mu(a, b, \lambda) = \mu(\lambda)$. The two equations of motion become

$$M_a \dot{v} = -F_N \mu(\lambda) \tag{7}$$

$$J_w \dot{\omega} = rF_N \mu(\lambda) - T_b \tag{8}$$

3.3. Friction Coefficient

The slip ratio, λ, is the control input given to the local controller, which will generate the braking torque the wheel uses to stop the aircraft. It is defined as the ratio of the angular speed of the wheel to the velocity of the aircraft, with the embedded equation:

$$\lambda_i = \frac{v - \omega_i r}{v} \tag{9}$$

where v is the velocity of the aircraft, ω_i is the angular speed of the ith wheel of the main landing gear of the aircraft. The differentiation of (9) is

$$\dot{\lambda}_i = -\frac{r\dot{\omega}_i}{v} + \frac{r\omega_i \dot{v}}{v^2} \tag{10}$$

substituting $\dot{v}$ and $\dot{\omega}_i$ from (7) and (8), respectively, in (10)

$$\dot{\lambda}_i = \frac{rT_b}{J_\omega v} - \frac{r^2 F_N \mu_i(\lambda_i)}{J_\omega v} - \frac{r\omega_i F_N \mu_i(\lambda_i)}{v^2 M_a} \tag{11}$$

This slip ratio, λ_i, has a value of $\lambda_i \in (0, 1]$, where 1 means the wheel is fully locked. The lateral friction coefficient μ_i is defined next, which is a non-linear function of the slip ratio λ_i, where μ_i can be defined as [30]

$$\mu_i(\lambda_i) = \alpha_i(1 - \exp^{-\lambda_i \beta_i}) - \gamma_i \lambda_i \tag{12}$$

where $\alpha_i, \beta_i, \gamma_i$ are the parameters dependent on the runway conditions and are given in Table 2.

Table 2. Values of parameter $\alpha_i, \beta_i, \gamma_i$ under different runway conditions [30].

Runway Condition	α	β	γ
Dry (asphalt)	1.28	23.99	0.52
Dry (Cobblestone)	1.37	6.46	0.67
Wet (asphalt)	0.86	33.82	0.35
Snow	0.19	94.13	0.06
Ice	0.05	306.39	0.0

The function of the friction coefficient in terms of slip ratio is plotted in Figure 4. The slip ratio controls the amount of friction available to the wheel. It can also be noted that the maximum friction available to the wheel is available at similar λ values regardless of the runway conditions.

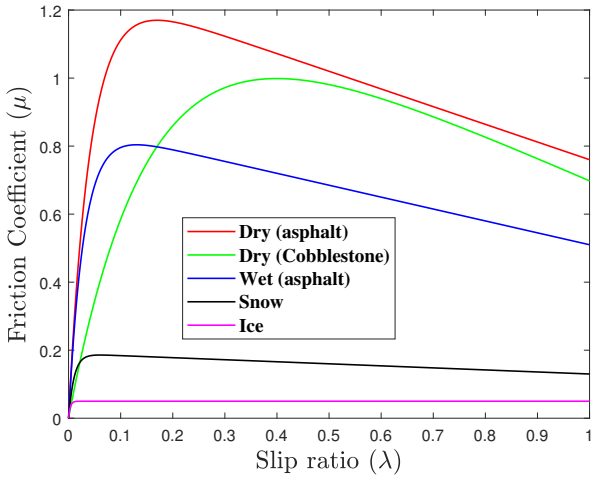


Figure 4. $\mu - \lambda$ curve under different runway conditions.

3.4. Braking Torque Controller Design

To stop the aircraft, the braking torque T_b is applied to exert force on the wheels with the help of friction. We set a desired slip ratio λ_d by which we can adjust the friction available to the wheel from the runway. We then measure the wheel speed and calculate the current slip ratio λ_i. To get the wheel to a speed close to the desired slip ratio, we use a sliding-mode controller (SMC) to control the slip ratio of the wheel, as it has good anti-locking performance and has strong robustness to changes in model parameters and control objectives [31]. To track the current slip ratio λ_i to the desired slip ratio, λ_d a sliding surface is defined as

$$s = \lambda_d - \lambda_i \tag{13}$$

The sliding surface is defined in the design of the SMC to regulate the slip ratio λ_i. A block diagram of the controller is shown in Figure 5. To overcome the disadvantage of chattering problems in SMC, an exponential approach law is adopted and is defined as [31]

$$\dot{s} = -\epsilon sgn(s) - Ks\epsilon > 0, K > 0 \tag{14}$$

where ϵ and k are positive constants and $sgn(\cdot)$ is the sign function, defined as

$$sgn(s) = \begin{cases} 1 & s > 0 \\ -1 & s < 0 \end{cases} \tag{15}$$

Differentiating (13) and substituting (14) and (11) into (13) yields

$$-\epsilon sgn(s) - Ks = -\frac{rT_b}{J_\omega v} + \frac{r^2 F_N \mu_i(\lambda_i)}{J_\omega v} + \frac{r\omega_i F_N \mu_i(\lambda_i)}{v^2 M_a} \tag{16}$$

The control law of SMC (T_b) can be obtained from (16) as

$$T_b = rF_N \mu_i(\lambda_i) + \frac{J_\omega \omega_i F_n \mu_i(\lambda_i)}{M_a v} + \frac{J_\omega v}{r}[\epsilon sgn(s) + Ks] \tag{17}$$

The overall system stability is ensured through a hierarchical structure: the local SMC guarantees slip ratio convergence (Lyapunov stable), while the consensus layer ensures force synchronization. The stability analysis of the SMC can be seen in [31], and the reader can refer to the article for the Lyapunov stability analysis of the SMC.

The output of the SMC controller will be an error between the desired and actual slip ratio. The response to this error will generate the braking torque shown in Figure 5.

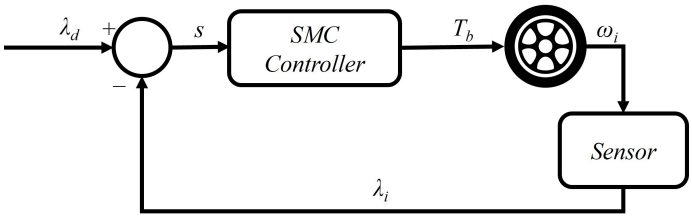


Figure 5. Local controller for braking torque.

4. Supervisory Consensus Control

We have discussed an aircraft's anti-skid brake control mechanism in Section 3. As one can see, the longitudinal force F_x acting on the wheel is significant and dependent on μ_i, which depends on the runway surface. Therefore, under a slight change in runway conditions, the aircraft will not follow the runway tracking path and might slip off the runway, which may cause an accident. To avoid this situation, we propose a supervisory control mechanism that will yield a consensus among the wheels so that all the wheels will experience the same longitudinal force, F_x, regardless of the runway condition. Therefore, in this section, we develop a consensus control mechanism in which the wheels on the left landing gear experience a different longitudinal force than the wheels on the right landing gear. However, the consensus control mechanism will output a common value of μ_c such that every wheel has the same force, which leads to adjusting the desired slip ratio coefficient λ_d. In practical aircraft braking systems, the control unit works centrally; however, the proposed framework adopts a distributed multi-agent abstraction. This is due to emerging WAIC architectures, where sensing and actuation may be physically distributed while logically coordinated. The proposed consensus controller can therefore be interpreted as either a distributed implementation or a modular extension of a centralized controller. For a wheel controller to develop a consensus among its neighbors, each wheel acts like an agent, and a connectivity matrix defines its connectivity with its neighbors. We will first describe the connectivity matrix using algebraic graph theory.

4.1. Algebraic Graph Theory

We use an undirected Graph G to represent the communication topology among the wheel agents. We define $G = \{V, E, A\}$ where $V = \{v_1, v_2, \ldots, v_n\}$ is the vertex set representing N wheels. E is the set representing the communication links between the wheel agents. E_{ij} is the edge between two nodes (wheel agents) $(v_i, v_j), i, j \in \{1, 2, 3, \ldots, N\}, i \neq j$. If $E_{ij} \in E$, then v_i is neighbor to v_j and they can communicate with each other. The

adjacency matrix is $A = [a_{ij}] \in R^{N \times N}$ with $a_{ij} = 1$ when i is connected to j, or $a_{ij} = 0$ otherwise. The in-degree matrix is a diagonal matrix with $S = diag\{s_1, s_2, \ldots, s_N\}$ with $s_i = \sum_{j \in N_i} a_{ij}$ where N_i is the number of control agents (wheel agents) connected to the ith control agent. The graph Laplacian matrix is $L = S - A$, where all row members add up to zero. L is a symmetric positive semi-definite matrix. The convergence rate (time for F_x consensus) will depend on the eigenvalues of L and is given by the second smallest eigenvalue of L. Let $L = [l_{ij}]_{N \times N}$ where $l_{ij} = l_{ii}$ on-diagonal, and $l_{ii} = \sum_{i \neq j} a_{ij}$ whereas l_{ij} off-diagonal is $l_{ij} = -a_{ij}$.

4.2. Consensus of Longitudinal Force

Assume we have wheels with longitudinal forces $\{F_{x1}, F_{x2}, F_{x3} \ldots F_{xn}\}$ trying to reach consensus. Each wheel is driven by its local controller, but its control input is fed forward from the supervisory consensus controller. Let $u_i(t)$ be the control input of the consensus controller. This input is defined as the sum of the differences of forces obtained from neighboring wheels to the ith wheel as defined in (19). This can be further represented with the Laplacian matrix L as in (20). To achieve consensus, we create a feedback control law u_i for each wheel that makes use of the information obtained over the communication network at sampling time t_k, $k = 0, 1, 2, \ldots$, and we suppose that for all initial conditions, $\lim_{t \to \infty}(F_{ix}(t) \rightarrow F_{ref}(t)), i, \in [1, N]$ where F_{ref} is a reference force. Furthermore, we assume that between any two consecutive control updates, the input of each wheel is held constant in a zero-order hold fashion equal to the last control update.

$$\dot{F}_{ix} = u_i(t) \tag{18}$$

where

$$u_i(t) = -\sum_{i,j \in N} \left(F_{ix} - F_{jx}\right) \tag{19}$$

or

$$u_i(t) = -LF_{ix} \tag{20}$$

The consensus control mechanism is depicted in Figure 6, where the local SMC controller will generate the slip ratio λ_i. The slip ratio will generate friction μ_i, exerting force on the wheel. The force F_x is given as an input to the consensus controller, and the consensus controller will generate a new μ_{ci}. From Equation (12), μ is a function of λ therefore, to achieve the μ_{ci} at each wheel, the λ_{di} needs to be updated to keep the longitudinal forces acting on the wheels the same.

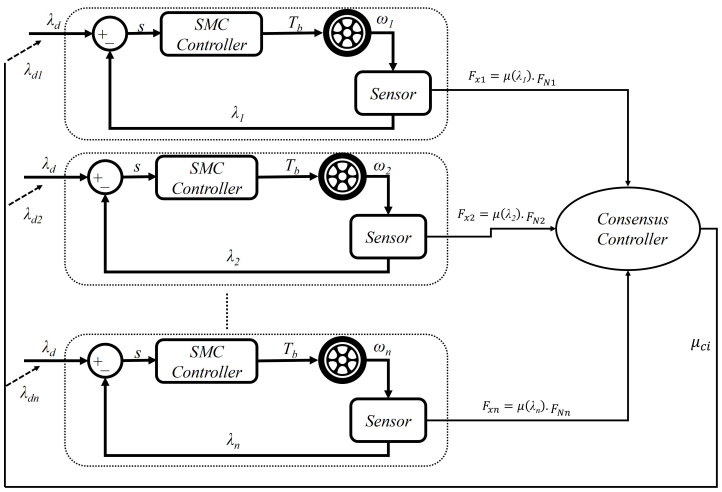


Figure 6. Supervisory consensus control.

5. Wireless Communication Model

To evaluate the consensus control mechanism, we consider a simple wireless communication system based on time-division multiple access [32] that mimics the wireless avionic intra-communication. This type of protocol assigns different time slots to sensor nodes. Nodes can send messages only in their time slot, thus eliminating contention. As the wireless channel is also shared between other devices such as radio altimeters, the consensus controller needs to perform a channel assessment before starting the time-slotted transmission to the wheel agents to avoid interference from devices of different systems. Once the channel is free, the controller will start the transmission; otherwise, it will back off and attempt it after a random time. The frequency at which the controller attempts to access the channel is the sampling time at which the consensus control algorithm will update its input.

In the first transmission slot, the consensus controller requests from each wheel agent the latest information about the wheel's friction force, μ_i. A wheel that receives a request will send the data (μ_i) to the controller in its scheduled time slot. Once the consensus controller receives the provided friction force information from the wheels, the controller estimates the friction force μ_{ci} which should act on each wheel and then broadcasts back, in the last slot, the desired slip ratio λ_{di} to the wheels as shown in Figure 7.

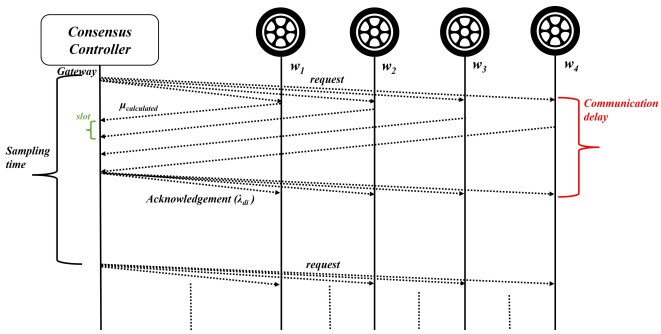


Figure 7. Wireless communication protocol.

According to this time-slotted access protocol, the communication delay between the transmissions of the controller request transmission and the consensus acknowledgment is the sum of all slot durations, i.e., $\sum_{N+2} st$, where st is the slot time, N is the number of sensors, and two slots are used for the controller broadcast. Since the controller broadcasts simultaneously to all sensors in a scheduled fashion, they experience the same delay. Hence, the delay can be designed to be shorter than the control system's sampling time, guaranteeing up-to-date information to the control system. Although this can limit the number of sensors, given the sampling time restriction, this scheduled access avoids packet collisions between sensors, improving reliability.

5.1. Communication Error Model

Due to the shared wireless channel resources with other systems (e.g., radio-altimeter, other wireless sensor networks), packets received at the consensus controller (friction data) and over the sensors at each wheel (controller request and/or consensus output) might contain errors due to inter-system interference. When the gateway request for data from the wheel is lost, the wheel sensor will not be triggered to transmit the latest friction information. Similarly, even if the request is successfully received and the sensor sends the friction data, that data might be lost due to interference or noise; therefore, the gateway has to be able to estimate the data it was expecting from the sensor. On the sensor side, when the consensus controller outputs the desired slip ratio and transmits it to each sensor, that packet might also be lost, and the sensor also has to estimate the control information. We can

also use machine learning-based methods to estimate μ_{est}, but these estimations are not in the scope of this paper. Therefore, we use a statistical abstraction of the estimation process by modelling the estimated values at the gateway and sensor sides as $\mu_{est} = \mu_{real} + \epsilon$, where ϵ is a normal distribution with a zero mean and σ the standard deviation, which will represent the estimation accuracy.

5.2. Realistic WAIC Channel Model

The wireless channel in WAIC systems is characterized by interference, fading, and strict reliability constraints as outlined in [33]. To incorporate these conditions, we consider two important improvements:

5.2.1. Path Loss and Fading

To include path loss and fading, the received signal is modeled using the wireless link budget model as:

$$P_{r,(\text{dBm})} = P_{t,(\text{dBm})} + G_{t,(\text{dBi})} + G_{r,(\text{dBi})} - L_{(\text{dB})}(d) + 20\log_{10}|h| \tag{21}$$

where P_r is the received power, P_t is the transmitted power by the sender, both measured in dBm, G_t represents the transmitted antenna gain and G_r represented the receiver gain both measured in dBi, $L(d)$ represent the path loss function. h is the channel fading gain. Due to the predominantly line-of-sight conditions in aircraft environments, the fading coefficient h is modeled using a Rician distribution. This captures both the deterministic line-of-sight component and multipath reflections from aircraft structures.

5.2.2. Packet Loss Model

To represent burst errors, packet loss is modeled using a two-state Gilbert–Elliott process. The channel switches between a good state with low packet loss and a bad state with significantly higher loss, capturing the effects of intermittent interference in avionics environments [34].

5.2.3. Communication Delay

The TDMA protocol ensures deterministic delay; however, additional delays may arise due to channel access and processing. The total delay is bounded by T_d, and its impact on control performance is evaluated in Section 5. Maintaining the delay below the control sampling interval is critical for the stability and performance of the consensus controller [35].

6. Numerical Results

6.1. Simulation Setup

We have validated our proposed approach with an example of 4 wheels on the main landing gear, two on the left side, and two on the right side of the aircraft. We use the simple SMC controller for anti-skid brake torque control and add our supervisory consensus control. The parameters used in the model are taken from [7] and are given in Table 3.

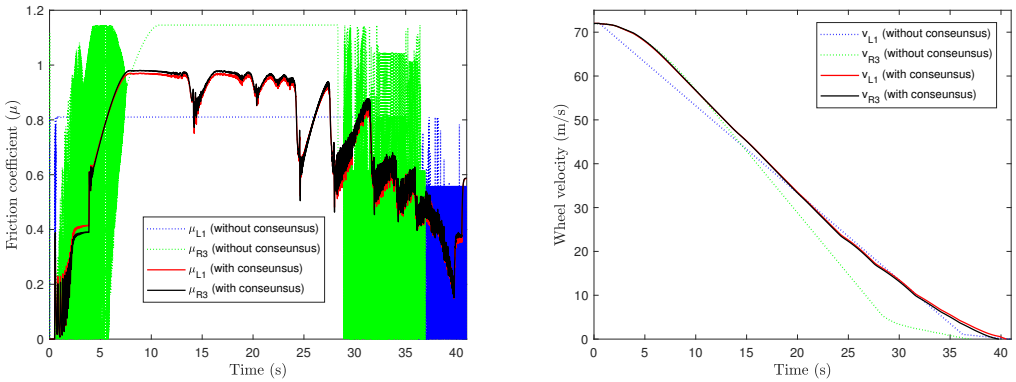
Table 3. Parameters of an aircraft [7].

Symbol	Parameter	Value
M_a	Aircraft weight (left, right)	18,118, 16,394 kg
g	Gravitational constant	9.81 m/s^2
r	Radius of the wheel	0.4 m
J_w	Rotational inertia of the wheel	1.885 kgm^2
J_a	Inertia of aircraft	6,141,855 kgm^2
l_l	Distance of left gear from axle	10 m
l_r	Distance of right gear from axle	10 m
v_0	Initial velocity of aircraft	72 m/s
dt	Sampling time	5 ms
st	Slot time	144 µs
T_d	Total communication delay	0.864 ms

6.2. Consensus with Perfect Communication

We will initially analyze the consensus model with perfect communication under varied runway conditions. The left side of the runway is wet, and the right is dry. For a loaded aircraft, the normalized force acting on the wheels might be different; therefore, the consensus control model needs to consider the load imbalance. To the best of our knowledge, this difference has not been reported anywhere, as airlines do not share load information due to security concerns. Therefore, an assumption needs to be made. Since the load weight is significantly lower than the aircraft weight, the impact of load imbalance is insignificant, so we assume a weight difference of 10% on the right and left landing gear. We observe the impact of the proposed consensus controller on the landing performance of the aircraft. We observe the friction coefficient on wheels w_{L1} on the left side of the landing gear and w_{R3} on the right side with and without the consensus controller in Figure 8a. The difference is rather significant without using a consensus controller because the left landing gear wheel (w_{L1}) is on the wet side, and the right landing gear wheel (w_{R3}) is on the dry side of the runway. This difference in friction force will cause a mismatch in the velocity of the wheels. To have a safe and smooth landing, we need to minimize the difference in the friction force, and the friction force acting on all the wheels must be equal. For that, we use our supervisory consensus controller, which will receive the actual friction forces acting on the wheels and estimate the equal amount of force that should act on each wheel. We need to adjust our desired slip ratios λ_{di} to generate those equal forces. Therefore, the consensus controller will output the estimated friction coefficient μ_{ci} for each wheel and the desired estimated slip ratio λ_{di}. This difference is reduced when we use the consensus controller, as shown in Figure 8a. The wheel velocity is shown in Figure 8b. Since the velocity of the left wheels w_{L1} and w_{L2} is the same and the velocity of the right wheels w_{R3} and w_{R4} is also the same, we only show the velocity of the wheels w_{L1} and w_{R3} in the figure. We can see from Figure 8b that the wheel velocity without consensus is different due to the difference in friction force available to the wheels, but the wheel velocity is very much the same when we use the consensus controller.

The larger friction force acting on the right landing gear (w_3, w_4) will generate a high drag torque T_a force on the aircraft, and the aircraft will tend to move away from the runway center line. The drag torque acting on the aircraft is shown in Figure 9. It is clear from the results that the drag force acting on the aircraft is significantly lower with consensus control as compared to without consensus control.



(**a**) (**b**)

Figure 8. Friction force and velocity of the wheels of the main landing gear. (**a**) Friction force acting on the wheels of the main landing gear. (**b**) Velocity of the wheels of the main landing gear.

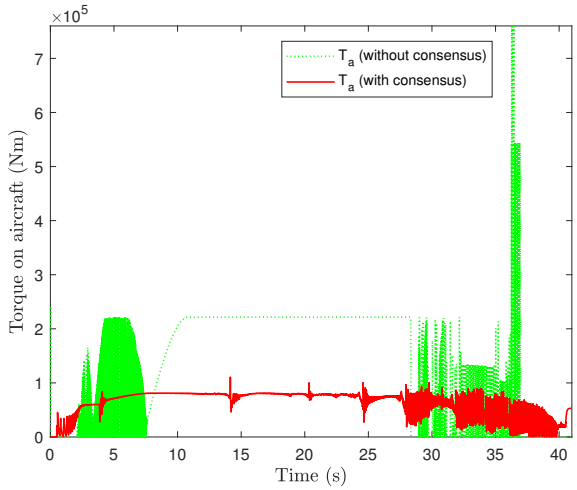


Figure 9. Drag torque acting on the aircraft.

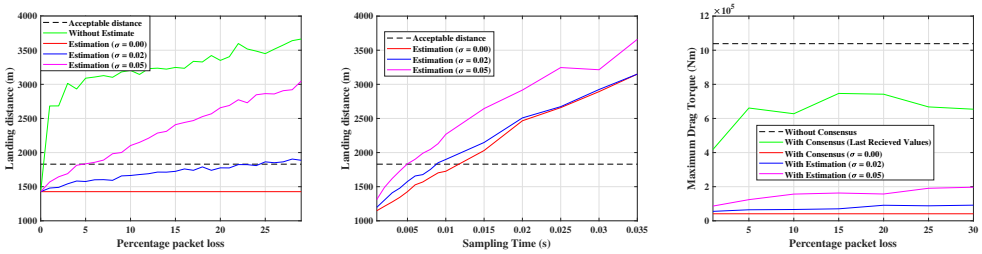
6.3. Consensus with Communication Losses

Following consensus control with perfect communication, we now examine the effects of transmission delays and packet loss due to wireless channel impairments on the landing distance. We initially chose a sampling time of 5 ms. When transmission losses increase, as shown in Figure 10a, the landing distance is significantly increased, even beyond a safe distance, when we are not estimating the slip ratio received from the neighbor wheels. To counteract the effects of packet loss, we propose estimating the lost values using a Normal distribution with zero mean. We tested different standard deviations σ and found that the best-fit estimation is with $\mathcal{N}(0, 0.02)$. This achieves an acceptable level of performance even though there were 25% communication losses (see Figure 10a).

We then looked at the performance of consensus control in terms of landing distance with varying the sampling time while keeping the losses constant (5%), as shown in Figure 10b. From the result, it is evident that the communication time interval (equal to the sampling time) also significantly affects the system performance. The sampling time will have to be chosen between 5 ms and 10 ms, depending on the interference losses, to achieve an acceptable landing distance.

We have also examined the maximum drag torque an aircraft experiences under wireless communication constraints. In Figure 10c, we can see that while keeping the sampling time of 5 ms the same for all simulations, the maximum drag an aircraft experiences without

consensus is very high but should ideally be zero, while consensus control results in much lower drag despite communication impairments, the drag torque is still not close to zero. However, with $\mathcal{N}(0, 0.02)$, the proposed estimation approach overcomes the impairments and results in similar control performance as perfect communication.



(**a**) (**b**) (**c**)

Figure 10. Effect of packet loss and sampling time on consensus control. (**a**) Effect of packet loss (Gilbert–Elliott model) on landing distance. (**b**) Effect of sampling time at 5% packet loss. (**c**) Maximum drag torque under burst packet loss and estimation.

6.4. Failure Limits Under Physical-Layer Impairments

We have looked at consensus control mechanism under communication loss in Section 6.3, and now we wanted to link these ratios with actual wireless channel model mentioned in Section 5, in order to identify the physical-layer conditions that may cause the consensus controller to fail.

In our TDMA scheme, a single sensor data packet of $L = 128$ bits is transmitted in a slot of $st = 144\,\mu s$ (Table 3). Under the Rician fading channel with K-factor $K = 10$ dB (a typical value for the predominantly line-of-sight WAIC environment [33]), the bit error probability for uncoded BPSK can be conservatively approximated by

$$P_b(\bar{\gamma}) \approx \frac{1}{2} \exp\left(-\frac{K}{K+1}\, \bar{\gamma} \right), \tag{22}$$

where $\bar{\gamma}$ is the average received SNR per bit. The corresponding packet error rate (PER) is $P_p = 1 - (1 - P_b)^L$, which feeds directly into the good-state loss probability P_g of the Gilbert–Elliott model. The bad-state loss probability is set to $P_b \approx 1$, and the steady-state probability of the bad state p_{bad} is determined by the duty cycle of strong interference (e.g., from radio-altimeter bursts). The average packet loss seen by the consensus controller is then

$$p_{\text{avg}} = (1 - p_{\text{bad}})\, P_g + p_{\text{bad}}\, P_b.$$

A log-normal shadowing component of $\sigma = 3$ dB is incorporated as an additional fade margin that shifts the required SNR upward by σ. LoS blockage is modelled as a periodic 20 dB attenuation; if the blockage interval is shorter than the TDMA frame ($T_d = 0.864$ ms) and does not coincide with the sensor's assigned slot, the time-slotted protocol inherently avoids the lost transmission.

Using the empirical relationship between packet loss and landing distance from Figure 10a (with the estimation error $\mathcal{N}(0, 0.02)$), we define a *failure condition* as the point where the landing distance exceeds 120% of the ideal consensus value. This corresponds to an average packet loss of approximately 20%. Solving (22) and the link budget for this threshold yields the following operational limits:

- Rician fading only($K = 10$ dB, no interference bursts): the system remains functional down to an average SNR of ≈5 dB.
- Rician fading + 3 dB shadowing: the required SNR rises to ≈8 dB.

- Bursty interference/LoS blockage: as long as the duty cycle of the bad state stays below 15%, the average packet loss remains under 20% and the system maintains acceptable performance.

These thresholds confirm that the proposed consensus control with Gaussian estimation is robust to realistic WAIC channel conditions and only fails when the average packet loss approaches 20%. The mapping also clarifies why the packet-loss-oriented study of Section 6.3 implicitly captures the effects of lower-level physical impairments.

7. Conclusions

In this article, we have studied an SMC-based anti-skid braking control mechanism to control the braking torque on the main landing gear of an aircraft. We have investigated the effects of variations in runway conditions on the friction force at each wheel. Different forces experienced at each wheel lead to drag on the aircraft, which can result in an aircraft drifting off the runway during landing or a much longer landing distance. We propose a supervisory consensus control approach to adjust the desired slip ratio at each landing gear wheel to eliminate the effects of runway conditions. The proposed consensus control works well even with left and right landing gear load imbalance. In our implementation, the consensus controller exchanges information over a wireless avionic intra-communication (WAIC) channel, which can result in packet losses and transmission delays. As part of our consensus controller design, we propose an estimation algorithm to compensate for communication losses. Our simulations demonstrate that the proposed consensus control approach can achieve a significantly reduced drag on the landing gear wheels and an acceptable landing distance range. The estimation approach makes the consensus controller robust against wireless communication impairments, allowing wireless communications for aircraft control and reducing cabling and aircraft weight.

Furthermore, by linking the physical-layer channel model to the measured packet loss rates, we have identified the SNR and blockage conditions under which the system remains safe—providing clear design margins for future WAIC deployments and demonstrating the robustness of the proposed estimation-based consensus approach.

Author Contributions: Conceptualization, Z.I.; Methodology, Z.I., F.F. and D.P.; Validation, F.F. and D.P.; Formal analysis, Z.I.; Data curation, Z.I.; Writing—original draft, Z.I.; Writing—review and editing, F.F. All authors have read and agreed to the published version of the manuscript.

Funding: This study was conducted at Collins Aerospace, Applied Research & Technology, Cork, Ireland, and was part-funded by the European Union's CleanSky2 Research and Innovation Programme ICO-Brake under grant No. 945535.

Data Availability Statement: The original contributions presented in this study are included in the article. Further inquiries can be directed to the corresponding author.

Conflicts of Interest: Author Fadhil Firyaguna was employed by the company Collins Aerospace. The remaining authors declare that the research was conducted in the absence of any commercial or financial relationships that could be construed as a potential conflict of interest.

References

1. International Telecommunication Union. *Technical Characteristics and Operational Objectives for Wireless Avionics Intra-Communications (WAIC)*; Technical Report ITU-R M.2197; ITU: Geneva, Switzerland, 2010.
2. Reiser, C.; Villani, E.; Cardoso-Junior, M.M. A novel approach to runway overrun risk assessment using FRAM and flight data monitoring. *Aeronaut. J.* **2024**, *128*, 2054–2072. [CrossRef]
3. Baskaran, S.; Sivaprakasam, S. Friction analysis of aircraft landing gears due to landing impact. *Proc. Inst. Mech. Eng. Part J J. Eng. Tribol.* **2022**, *236*, 274–283. [CrossRef]

4. Wang, Z.; Liu, X.; Sun, D.; Bai, N.; Qi, P.; Jiao, Z. A real-time maximum tire-road friction tracking control method for aircraft braking system with disturbance compensation. *IEEE/ASME Trans. Mechatronics* **2024**, *29*, 3649–3660. [CrossRef]
5. Xu, F.; Liang, X.; Chen, M.; Liu, W. Robust Self-Learning PID Control of an Aircraft Anti-Skid Braking System. *Mathematics* **2022**, *10*, 1290. [CrossRef]
6. Liu, C.; Liu, H.; Han, L.; Wang, W.; Guo, C. Multi-level coordinated yaw stability control based on sliding mode predictive control for distributed drive electric vehicles under extreme conditions. *IEEE Trans. Veh. Technol.* **2022**, *72*, 280–296. [CrossRef]
7. Chen, M.; Xu, F.; Liang, X.; Liu, W. MSD-Based NMPC Aircraft Anti-Skid Brake Control Method Considering Runway Variation. *IEEE Access* **2021**, *9*, 51793–51804. [CrossRef]
8. Pritchard, J. Overview of landing gear dynamics. *J. Aircr.* **2001**, *38*, 130–137. [CrossRef]
9. Kanungo, A.; Kumar, P.; Gupta, V.; Salim; Saxena, N.K. A design an optimized fuzzy adaptive proportional-integral-derivative controller for anti-lock braking systems. *Eng. Appl. Artif. Intell.* **2024**, *133*, 108556. [CrossRef]
10. D'Avico, L.; Tanelli, M.; Savaresi, S.M.; Airoldi, M.; Rapicano, G. An anti-skid braking system for aircraft via mixed-slip-deceleration control and sliding mode observer. In *Proceedings of the 2017 IEEE 56th Annual Conference on Decision and Control (CDC)*; IEEE: Melbourne, Australia, 2017; pp. 4503–4508.
11. Lopetegui, J.J.M.; Papa, G.; Morandini, M.; Tanelli, M. Data-Driven Modeling and Regulation of Aircraft Brakes Degradation via Antiskid Controllers. *IEEE Trans. Reliab.* **2022**, *72*, 889–899. [CrossRef]
12. Zhang, Z.; Yang, Z.; Zhou, G.; Liu, S.; Zhou, D.; Chen, S.; Zhang, X. Adaptive Fuzzy Active-Disturbance Rejection Control-Based Reconfiguration Controller Design for Aircraft Anti-Skid Braking System. *Actuators* **2021**, *10*, 201. [CrossRef]
13. Jiao, Z.; Wang, Z.; Sun, D.; Liu, X.; Shang, Y.; Wu, S. A novel aircraft anti-skid brake control method based on runway maximum friction tracking algorithm. *Aerosp. Sci. Technol.* **2021**, *110*, 106482. [CrossRef]
14. Olfati-Saber, R.; Fax, J.A.; Murray, R.M. Consensus and cooperation in networked multi-agent systems. *Proc. IEEE* **2007**, *95*, 215–233. [CrossRef]
15. Kong, L.; Lin, T.; Koloskova, A.; Jaggi, M.; Stich, S. Consensus control for decentralized deep learning. In *Proceedings of the International Conference on Machine Learning*; PMLR: Vienna, Austria, 2021; pp. 5686–5696.
16. Lin, G.; Li, H.; Ma, H.; Yao, D.; Lu, R. Human-in-the-loop consensus control for nonlinear multi-agent systems with actuator faults. *IEEE/CAA J. Autom. Sin.* **2020**, *9*, 111–122. [CrossRef]
17. Huang, M.; Hu, Z.; Wang, L. Optimal consensus control for heterogeneous nonlinear non-affine multi-agent systems with uncertain control directions. *ICIC Express Lett.* **2022**, *16*, 177–185.
18. Ning, B.; Han, Q.L.; Zuo, Z.; Ding, L.; Lu, Q.; Ge, X. Fixed-Time and Prescribed-Time Consensus Control of Multi-Agent Systems and Its Applications: A Survey of Recent Trends and Methodologies. *IEEE Trans. Ind. Inform.* **2022**, *19*, 1121–1135. [CrossRef]
19. Wu, X.; Mao, B.; Wu, X.; Lu, J. Dynamic event-triggered leader-follower consensus control for multiagent systems. *SIAM J. Control Optim.* **2022**, *60*, 189–209. [CrossRef]
20. Singhal, A.; Vu, T.L.; Du, W. Consensus Control for Coordinating Grid-Forming and Grid-Following Inverters in Microgrids. *IEEE Trans. Smart Grid* **2022**, *13*, 4123–4133. [CrossRef]
21. Geranmehr, B.; Khanmirza, E. Optimal consensus control of multi-agent systems based on the state-dependent riccati equation. *Proc. Inst. Mech. Eng. Part C J. Mech. Eng. Sci.* **2022**, *236*, 9270–9281. [CrossRef]
22. Ijaz, Z.; Noor-A-Rahim, M.; Pesch, D. Leader–Follower-Based Self-Triggered Consensus Control of Industrial Induction Motor Drives. *IEEE Syst. J.* **2022**, *16*, 5917–5927. [CrossRef]
23. Sun, F.; Wu, X.; Kurths, J.; Zhu, W. Group consensus of heterogeneous multi-agent systems with packet loss and unknown speed of second-order agents in cooperative–competitive networks. *Nonlinear Dyn.* **2022**, *110*, 3447–3461. [CrossRef]
24. Zhao, G.; Hua, C. Sampled-Data Leaderless and Leader-Following Consensus of Multiagent Systems Under Nonidentical Packet Losses. *IEEE Trans. Netw. Sci. Eng.* **2021**, *9*, 795–806. [CrossRef]
25. Zhao, Y.; Wu, Z.; Li, F.; Yang, T.; Yang, C.; Gui, W. Design and implementation of Fuzzy-Mode-Based fault isolation and fault-Tolerant control for aircraft electric braking systems. *IEEE Trans. Autom. Sci. Eng.* **2025**, *22*, 12297–12308. [CrossRef]
26. Lyu, Z.; Gao, Y.; Chen, J.; Du, H.; Xu, J.; Huang, K.; Kim, D.I. Empowering intelligent low-altitude economy with large AI model deployment. *IEEE Wirel. Commun.* **2025**, *33*, 64–72. [CrossRef]
27. Shi, Y.L.; Liu, Z.W. Distributed impulsive control for secure consensus of nonlinear dynamical networks with node delay under denial-of-service attacks. *Asian J. Control* **2022**, *24*, 594–604. [CrossRef]
28. Yang, J. Deep Learning-Based Consensus Control of a Multi-Agents System with Unknown Time-Varying Delay. *Electronics* **2022**, *11*, 1176. [CrossRef]
29. Daidzic, N.E. Modeling and Computation of the Maximum Braking Energy Speed for Transport Category Airplanes. *J. Aviat. Technol. Eng.* **2017**, *6*, 1. [CrossRef]
30. Piccinini, M.; Zumerle, M.; Betz, J.; Papini, G.P.R. A Road Friction-Aware Anti-Lock Braking System Based on Model-Structured Neural Networks. *IEEE Open J. Intell. Transp. Syst.* **2025**, *6*, 522–536. [CrossRef]

31. Guo, J.; Jian, X.; Lin, G. Performance evaluation of an anti-lock braking system for electric vehicles with a fuzzy sliding mode controller. *Energies* **2014**, *7*, 6459–6476. [CrossRef]
32. Mystica, K.J.; Manickam, J.M.L. Learning to allocate: A delay and temperature-aware slot allocation framework for WBAN with TDMA-MAC. *Wirel. Netw.* **2025**, *31*, 165–183. [CrossRef]
33. Park, P.; Di Marco, P.; Nah, J.; Fischione, C. Wireless avionics intracommunications: A survey of benefits, challenges, and solutions. *IEEE Internet Things J.* **2020**, *8*, 7745–7767. [CrossRef]
34. Wang, T.; Liu, T.; Li, Y.; Zhao, J.; Gao, R.; Wu, S.; Pan, J. Packet Loss Modeling and Forward Erasure Correction for LEO Satellite Networks. *IEEE Trans. Commun.* **2026**, *74*, 3999–4013. [CrossRef]
35. Chen, Y.; Cong, Y.; Wang, X.; Sun, Z. Reliable Formation Under TDMA Mechanism: Control-Communication Codesign. *IEEE Trans. Syst. Man Cybern. Syst.* **2026**, *56*, 3099–3112. [CrossRef]

Disclaimer/Publisher's Note: The statements, opinions and data contained in all publications are solely those of the individual author(s) and contributor(s) and not of MDPI and/or the editor(s). MDPI and/or the editor(s) disclaim responsibility for any injury to people or property resulting from any ideas, methods, instructions or products referred to in the content.